Using Phase Congruency Model for Microaneurysms Detection in Fundus Image

Zhitao Xiao[1], Fang Zhang[1], Lei Geng[1], Jun Wu[1], Xinpeng Zhang[1], Long Su[2] and Chunyan Shan[3]
[1]*School of Electronics and Information Engineering, Tianjin Polytechnic University, Tianjin 300387, China*
[2]*Tianjin Medical University Eye Hospital, Tianjin 300384, China*
[3]*Tianjin Medical University Metabolic Disease Hospital, Tianjin 300070, China*

Keywords: Microaneurysms, Phase Congruency, Directional Cross-Section Profiles, Diabetic Retinopathy.

Abstract: This paper addresses an automatic detection method of microaneurysms in color fundus images, which plays a key role in computer assisted diagnosis of diabetic retinopathy, a serious and frequent eye disease. The main concentration of this paper is to detect microaneurysms with phase congruency. The first step consists in image normalization and green channel extraction. The second step aims at obtaining microaneurysms candidate regions, which is achieved using phase congruency. Then the irrelevant information, such as the vessel fragments, is removed by constructing directional cross-section profiles. Through testing on 50 fundus images provided by ROC website, the experimental results show that this method can accurately get microaneurysms in color fundus images.

1 INTRODUCTION

Diabetic retinopathy (DR) is a complication of diabetes that results from damage to the blood vessels of the light-sensitive tissue at the back of the eye (retina). It is a sight-threatening disease that possibly leads to vision impairment and blindness. It has been shown that an automated DR screening system would be a great assist in the processes of diagnosing and progression tracking. Microaneurysm (MA) is the swelling of the capillary caused by a weakening of the vessel wall, which appears as the tiny and reddish isolated dot. MAs are amongst the first clinical signs of the presence of DR. Hence, the automatic detection of MAs in color fundus images is critical for diagnosing the process of Diabetes and plays an important role on mass DR screening.

In section 2 we will briefly review the available methods for fundus images MAs detection, after which in section 3 phase congruency theory is introduced. The proposed method is described in details in section 4. Finally, the experiment results and conclusion of our method are presented in section 5 and section 6.

2 STATE-OF-THE-ART MA DETECTORS

MAs are characterized by their diameter which is always smaller than 125μm. They have typically low contrast and may be hard to distinguish from noise or pigmentation variations. In addition, color fundus images often suffer from non-uniform illumination, poor contrast and noise. Therefore, achieving efficient detection of MAs becomes a complex and challenging issue. Existing MAs detection algorithms can be divided into three categories, mathematical morphology methods (Spencer, 1996; Hipwell, 2000; Fleming, 2006; Walter, 2007), supervised learning based methods (Sinthanayothin, 2002; Niemeijer, 2005; Zhang, 2010), and filter based methods (Quellec, 2008; Hatanaka, 2012). Spencer et al. (Spencer, 1996) described a mathematical morphology based detection method for MAs. Using shade-correction and top-hat transformation, they gave satisfactory results. Whereas it is in fluorescein angiographies images and not appropriate for color fundus images. To detect the MA candidates in color fundus photographs, Niemeijer et al. (Niemeijer, 2005) presented a hybrid scheme that uses both the top-hat transformation and the supervised pixel

Xiao Z., Zhang F., Geng L., Wu J., Zhang X., Su L. and Shan C..
Using Phase Congruency Model for Microaneurysms Detection in Fundus Image.
DOI: 10.5220/0005186801580163
In *Proceedings of the International Conference on Pattern Recognition Applications and Methods* (ICPRAM-2015), pages 158-163
ISBN: 978-989-758-077-2

classification based method. Zhang et al. (Zhang, 2010) proposed a method based on Sparse Representation Classifier (SRC). Hatanaka et al. (Hatanaka, 2012) achieved automatic detection in non-dilated fundus images using the double-ring filter and the artificial neural network (ANN).

Although these methods described above have achieved automatic detection of MAs in different kinds of fundus images, there are still some problems, such as high false detection rate, high missing detection rate, and complex operation. The fundamental reason is that these approaches mainly use gradient information to describe image. Gradient based detection methods are sensitive to the contrast of image and noise. Thus such algorithms require initial images with high quality. If the fundus images are degraded due to the non-uniform illumination or low contrast, these methods will have difficulties to detect the real MAs and exclude a large number of non-MA objects. And the system will be more complex in further classification based on the region feature. On the whole, gradient-based approaches are difficult to achieve good detection results for fundus images with complex background.

Phase information is consistent with human visual system perception characteristics. It has many advantages in image description, such as invariance to contrast and brightness, high noise immunity. Therefore this article describes a novel MAs detection method based on phase information. Because phase information is invariant to contrast and brightness, it needs no enhancement preprocessing. Moreover, the proposed method detects MAs directly, which avoids the complex process of feature training and object classification. As a result, it greatly reduces the complexity and running time. The performance of the proposed method is demonstrated through experiments.

3 PHASE CONGRUENCY MODEL

Phase Congruency model (PC) is an image feature detector (Morrone, 1987; Xiao, 2004). It assumes the most accordant point of phase in Fourier component as the feature points, which can be used to detect step feature, line feature and roof feature.

PC has been successfully applied to texture segmentation, edge detection, image denoising and other fields with satisfactory results. Using PC for marking feature has significant advantages over gradient-based methods. It is invariant to image brightness and contrast. Hence it provides an absolute measurement of the significance of feature points, which accords to human visual perception characteristics. These excellent features make it ideal for medical images with various characteristics.

4 METHOD OF MA DETECTION IN FUNDUS IMAGE BASED ON PHASE CONGRUENCY

The proposed method is divided into three processes: preprocessing, getting MA candidates, and screening MAs. The flowchart of this method is illustrated in Figure 1.

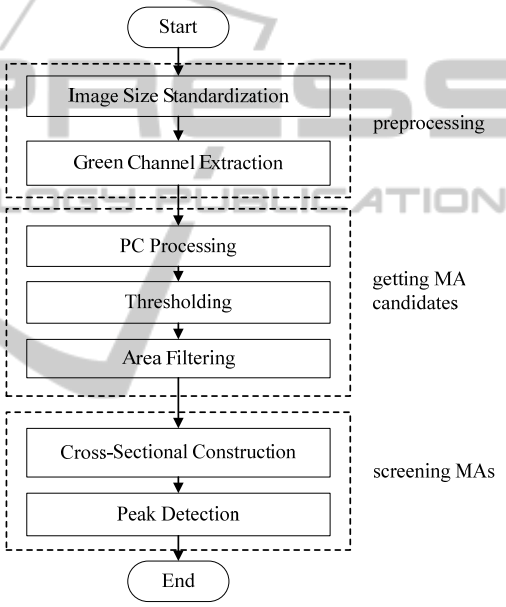

Figure 1: Flowchart of MAs detection in fundus image based on PC.

4.1 Preprocessing

Firstly, for setting the parameters conveniently, the images are resized to horizontal resolution 768 pixels using bicubic interpolation. Compared with the red and blue channels, the objects such as blood vessels and MAs in the retinal layer are best represented (see Figure 2) in the green channel. Therefore, the green channel of the color fundus image is chosen for the subsequent processing. In the green channel of color fundus image, MAs appear as dark patterns, small, isolated and circular shape, as shown in Figure 3.

(a) original image; (b) green channel.

Figure 2: Original image and its green channel image.

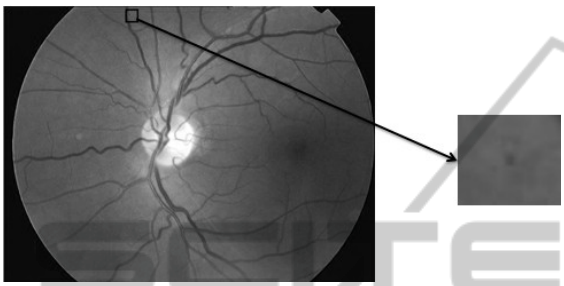

Figure 3: MA details in green channel.

4.2 MA Candidates Detection

4.2.1 Objects Detection based on PC

Here, we use the PC calculating method provided by Kovesi (Kovesi, 1999), which extended the 1-D PC to allow the calculation of 2-D PC of image by applying 1-D analysis over several orientations and scales. After PC calculation, a pattern mask is chosen to eliminate the boundary of the image. The PC detection result is shown in Figure 4 (Because the image has low gray value after PC processing, in order to demonstrate the result of PC clearly, the image is shown with gray enhancement). The structures which have large local energy (including MAs) are preserved, while blood vessels and other large lesions have been filtered out mostly.

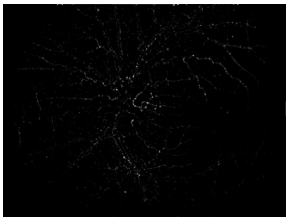

Figure 4: Detection result from PC.

4.2.2 MA Candidates Detection

After feature detection by PC, points with high gray-scale correspond to the targets with salient features in green channel fundus image. Thus, MA candidates can be extracted by thresholding. Here, one-tenth of the maximum gray value in the PC detection result is selected as the threshold to achieve binarization for Figure 4. Then the area filtering is executed, through which large structures (blood vessels and other large lesions) and small structures (noise) are removed, and the MA candidates (including some false MAs and the real MAs) are left. Figure 5 shows the filtered results superimposed on the green channel image. We can see that most of the MA candidates occur on the blood vessels. Some corners and junctions of blood vessels, which have similar brightness and shape with MAs, lead to error detection. With the knowledge of pathology, MAs are located on capillaries. And as these capillaries are not visible in color fundus images, MAs should appear as isolated patterns. Based on these characteristics, false MAs can be wiped away (shown in next Section).

Figure 5: MA candidates superimposed on the green channel image.

4.3 Cross-Section Construction

According to the shape feature of MA candidates, non-MA targets can be excluded. For each MA candidate point (x,y), a $W\times W$ neighborhood window centered on (x,y) is taken at the original green channel image (W=2L−1. L is considered according to the image resolution. Here, L=8 is selected corresponding to the image horizontal resolution of 768 pixels). In the selected neighborhood, eight scanning lines with different angles passing through the center point are tested (here, they are 0°, 22°, 45°, 66°, 90°, 111°, 135°, 156°). The records of the pixel gray values along the eight scanning lines constitute a set of one dimensional intensity profiles, in other words, form a set of cross-section profiles (Lazar, 2013). Vessel segments, background regions and MAs have different characteristics, as shown in Figure 6. It is found that MAs show significant Gaussian-like peaks for all directions. While in the case of the blood vessels, only the profiles of scanning lines cross the vessel show clear peaks. As

the directions of the scanning lines approximate to the direction of the vessel segment, the peaks of the profiles become more and more unclear, until almost completely disappears.

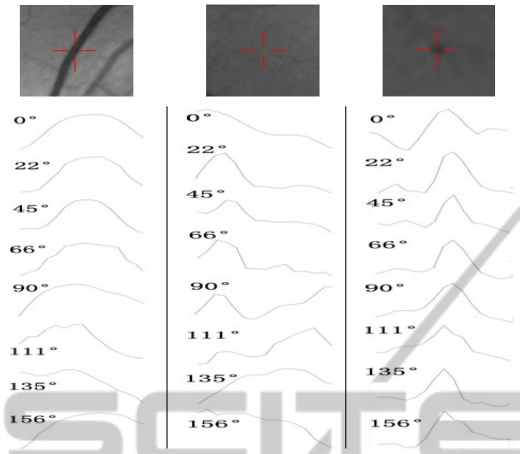

(a)vessel segment; (b)background region; (c)MA.

Figure 6: Cross-section profiles of a vessel segment, background region and an MA.

Peak detection is applied on each profile. Several parameters for the peaks, including size, height, and shape are calculated subsequently. Once a peak is detected at the center of the window, the slope between adjacent pixels is calculated. Thereby the four special points of the peak are determined. Specifically, the values of inc_s and inc_e correspond to the start and the end indices of the increasing ramp. Similarly, dec_s and dec_e denote the boundaries of the decreasing ramp, respectively. Figure 7 shows a graphical interpretation of the ramps. Then the following five properties of each peak are calculated using these four points.

(1) The peak width is the difference between the start and the end indices of the peak:

$$w_{peak}(i) = dec_e(i) - inc_s(i) \tag{1}$$

(2) The top width is the size of the gap between the increasing and the decreasing ramp:

$$w_{top}(i) = dec_s(i) - inc_e(i) \tag{2}$$

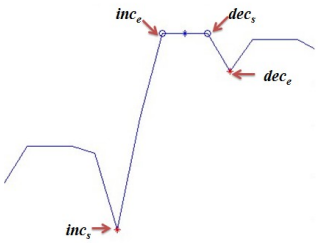

Figure 7: Four special points of peak detection.

(3) The average ramp height:

$$Rheights(i) = \left[h_{inc}(i) + h_{dec}(i)\right]/2 \tag{3}$$

where

$$h_{inc}(i) = P[inc_e(i)] - P[inc_s(i)] \tag{4}$$

stands for the increasing ramp height, and

$$h_{dec}(i) = P[dec_s(i)] - P[dec_e(i)] \tag{5}$$

is the decreasing ramp height, $P[\cdot]$ denotes the gray value of a given pixel;

(4) The average ramp slope:

$$Rslopes(i) = \left[S_{inc}(i) + S_{dec}(i)\right]/2 \tag{6}$$

where

$$S_{inc}(i) = h_{inc}(i)/\left|inc_e(i) - inc_s(i)\right| \tag{7}$$

is the increasing ramp slope, and

$$S_{dec}(i) = h_{dec}(i)/\left|dec_e(i) - dec_s(i)\right| \tag{8}$$

is the decreasing ramp slope;

(5) The peak height is computed as the difference between the intensity of the center pixel and a baseline that connects the start and the end of the profile:

$$h_{peak}(i) = \frac{P[L] - (P[dec_e(i)] - P[inc_s(i)])}{w_{peak}(i) \times [L - inc_s(i)] + P[inc_s(i)]} \tag{9}$$

where i=0,1,2,...,7, represents the eight scanning directions. After obtaining the five properties, *Score* is calculated by the following equation, which has considered the shape, symmetry, sharpness and contrast of the candidates.

$$Score = \frac{M_{h_{peak}} \times \mu_{Rslopes}}{1 + \sigma_{w_{peak}} + \sigma_{w_{top}} + \sigma_{Rslopes} + \sigma_{Rheights} + \sigma_{h_{peak}}} \tag{10}$$

where $M_{h_{peak}}$ is the minimum of h_{peak}, $\mu_{Rslopes}$ is the mean of *Rslopes*, $\sigma_{w_{peak}}$ is the standard deviation of w_{peak}. Similarly, $\sigma_{w_{top}}$, $\sigma_{Rheights}$, $\sigma_{Rslopes}$ and $\sigma_{h_{peak}}$ are the standard deviation of w_{top}, *Rheights*, *Rslopes* and h_{peak}, respectively.

By calculating the *Score* of a large of real MAs, we get the *Score* value range as [20, 30] for the real MAs. Accordingly, when the candidate's *Score* value falls into this range, it can be considered as the real MA. Otherwise, it will be treated as the false target and be removed away.

5 RESULTS AND DISCUSSION

5.1 Materials and Results

To examine the performance of the proposed method, we utilize the fundus images provided by Retinopathy Online Challenge (ROC) website (Retinopathy Online Challenge, 2008). The ROC provides 50 training cases and 50 test cases, in which "gold standard" locations of MAs are provided for the training cases, and the MAs in the test ones are not labeled. In the experiment, the computerized scheme is developed using the training set, and the performance of the proposed method is validated with "gold standard". Figure 8 shows the MAs detection results of three images from the training set, where (a1), (a2) and (a3) are the "gold standard" given by ROC, (b1), (b2) and (b3) are the final MAs detection results of our method. There are uneven illumination and low contrast problems in (a1) and (a2). Although the image quality of the three selected fundus pictures are different, experimental result shows that the proposed method can detect the MAs accurately in color fundus images without any enhancement processing.

5.2 Quantitative Evaluation and Comparison

In the image level, the detection sensitivity, specificity and accuracy are selected as the algorithm stability criteria, which are defined as the following formulas (Gao, 2012):

$$sensitivity = \frac{TP}{TP + FN}$$

$$specificity = \frac{TN}{TN + FP}$$

$$accuracy = \frac{TP + TN}{TP + TN + FP + FN}$$

where TP means true positive, FP is false positive, TN stands for true negative, and FN notes false negative.

In this paper, 50 fundus images in training set are detected. To the image level, the method achieved sensitivity of 94%, specificity of 100%, and accuracy of 96%, respectively. Experimental data show that this method can give good performance in detecting MAs in color fundus images, which also obtain satisfactory results for distinguishing between normal and diseased fundus images.

Table 1 shows the sensitivity of different methods at 1.0 FP per image (that is, the sensitivity when the number of False Positive is 1.0). Sensitivity is the number of true MAs correctly detected, while false positive is the number of non-MAs detected as MAs. Table 1 demonstrates the performance of the proposed method and some existed methods. From Table 1, one can see that our method can precisely locate MAs with high sensitivity at low false positive rate.

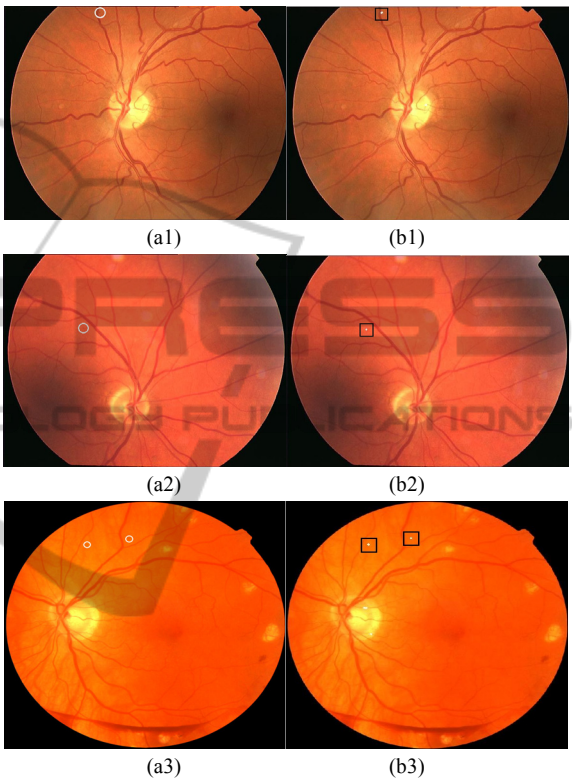

(a1), (a2), (a3) are MAs labeled by ROC (MAs are circled); (b1), (b2), (b3) are the MAs detection results of the proposed method (white dots in squares are detected MAs).

Figure 8: MAs detection results of the proposed method.

Table 1: Comparison of the sensitivity at 1.0 FP per image.

	Sensitivity at 1.0 FP
Niemeijer (Niemeijer, 2005)	0.018
Math Morph (Spencer, 1996)	0.072
SRC (Zhang, 2010)	0.13
double-ring (Hatanaka, 2012)	0.15
Proposed Method	0.23

6 CONCLUSIONS

This paper proposes a novel MAs detection method in color fundus image based on phase information,

which including three processes, i.e. preprocessing, getting MA candidates, and screening MAs. The PC model is used to get MAs candidates. The obtained MAs candidates are very near to the true MAs, which give the good basis for next processing. Then, the irrelevant information, such as the vessel fragments, is removed by constructing directional cross-section profiles. This approach is invariant to image contrast and brightness, which needs no enhancement processing. The experiments results on 50 images provided by ROC website show that this method can accurately detect microaneurysms in color fundus images.

ACKNOWLEDGEMENTS

This work was supported by the National Nature Science Foundation of China (NSFC) under grant No. 61102150 and the Tianjin Science and Technology Supporting Projection under grant No. 13ZCZDGX02100.

REFERENCES

Spencer, T., Olson, J. A., McHardy, K. C., et al, 1996. An image-processing strategy for the segmentation and quantification of microaneurysms in fluorescein angiograms of the ocular fundus [J]. *Computers and Biomedical Research*, 29(4): 284-302.

Hipwell, J. H., Strachant, F., Olson, J. A., et al, 2000. Automated detection of microaneurysms in digital red-free photographs: *A diabetic retinopathy screening tool* [J]. *Diabetic Medicine*, 17(8): 588-594.

Fleming, A. D., Philip, S., Goatman, K. A., et al, 2006. Automated microaneurysm detection using local contrast normalization and local vessel detection [J]. *IEEE Transactions on Medical Imaging*, 25(9):1223-1232.

Walter, T., Massin, P., Erginay, A., et al, 2007. Automatic detection of microaneurysms in color fundus images [J]. *Medical Image Analysis*, 11(6): 555-566.

Sinthanayothin, C., Boyce, J. F., Williamson, T. H., et al, 2002. Automated detection of diabetic retinopathy on digital fundus images [J]. *Diabetic Medicine*, 19(2):105-112.

Niemeijer, M., Ginneken, B., Staal, J., et al, 2005. Automatic detection of red lesions in digital color fundus photographs [J]. *IEEE Transactions on Medical Imaging*, 24(5): 584-592.

Zhang, B., Karray, F., Zhang, L., et al, 2010. Microaneurysm (MA) detection via sparse representation classifier with MA and Non-MA dictionary learning [C]. In *IEEE International Conference on Pattern Recognition*, 277-280.

Quellec, G., Lamard, M., Josselin, P. M., et al, 2008. Optimal wavelet transform for the detection of microaneurysms in retina photographs [J]. *IEEE Transactions on Medical Imaging*, 27(9): 1230-1241.

Hatanaka, Y., Inoue, T., Okumura, S., et al, 2012. Automated microaneurysm detection method based on double-ring filter and feature analysis in retinal fundus images[C]. In *25th International Symposium on Computer-Based Medical Systems*. Rome, 1-4.

Morrone, M. C., Owens, R. A., 1987. Feature detection from local energy [J]. *Pattern Recognition Letters*, 6(5): 303-313.

Xiao, Z. T., Hou, Z. X., 2004. Phase based feature detector consistent with human visual system characteristics [J]. *Pattern Recognition Letters*, 25(10): 1115-1121.

Kovesi, P., 1999. Image features from phase congruency [J]. Journal of Computer Vision Research, 1(3): 1-26.

Lazar, I., Hajdu, A., 2013. Retinal Microaneurysm detection through local rotating cross-section profile analysis [J]. *IEEE Transactions on Medical Imaging*, 32(2): 400-407.

Retinopathy Online Challenge, 2008. http://roc.health-care.uiowa.edu/.

Gao, W. W., Shen, J. X., Wang, Y. L., 2012. Efficient and automated detection of microaneurysms from non-dilated fundus images [J]. *Chinese Journal of Biomedical Engineering*, 31(6):839-845.